Available online at www.sciencedirect.com
ScienceDirect
Catalysis Today 136 (2008) 136–145
CATALYSIS TODAY
www.elsevier.com/locate/cattod

Regeneration mechanism of $Pt/BaO/Al_2O_3$ lean NO_x trap catalyst with H_2

S.S. Mulla [a], S.S. Chaugule [a], A. Yezerets [b], N.W. Currier [b], W.N. Delgass [a], F.H. Ribeiro [a,*]

[a] *School of Chemical Engineering, Purdue University, Forney Hall of Chemical Engineering, 480 Stadium Mall Drive, West Lafayette, IN 47907-2100, United States*
[b] *Cummins Inc., 1900 McKinley Avenue, Columbus, IN 47201, United States*

Available online 3 March 2008

Abstract

Regeneration of a $Pt/BaO/Al_2O_3$ NO_x storage-reduction catalyst was studied using H_2 as a model reductant. We propose that the regeneration process involves a localized reaction front of the reductant that travels through the catalyst bed with complete regeneration of the trapping sites. When NH_3 was used as a regenerating gas instead of H_2, the process was found to be equivalent to that with H_2, and NH_3 was found to be as effective as H_2 in regenerating the trap catalyst. The process was limited only by the supply of the hydrogen atoms, irrespective of the source of hydrogen (H_2 or NH_3) and was also not affected by temperature changes or by the presence of CO_2 and H_2O. Even though Pt by itself is not very selective in reducing the NO_x to N_2 in a NO_x/H_2 feed stream, a high N_2 selectivity is maintained over the Ba-containing trap catalyst since the undesirable byproducts, mainly NH_3, continue to react further until they are optimally converted to N_2. In fact, we propose that the regeneration of the trap catalyst using H_2 as the reductant involves the formation of NH_3 as an intermediate from the stored NO_x, and NH_3 acts as a carrier of H-atoms. The NH_3 ultimately gets further oxidized to N_2 by the stored NO_x, the oxygen source on the catalyst, giving high selectivity towards N_2.

Keywords: Regeneration of lean NO_x traps; $Pt/BaO/Al_2O_3$ NO_x traps; Ammonia as a NO_x reduction intermediate

1. Introduction

The concern for reducing the energy consumption without inhibiting the economic growth has brought the vehicular engine fuel economy under increasing scrutiny. Lean-burn engines, *e.g.*, diesel engines, exhibit better fuel efficiency than those operating near stoichiometric air to fuel ratios, *e.g.*, gasoline engines, and hence the use of diesel engines in passenger vehicles is expected to increase relative to gasoline engines. On the other hand, upcoming environmental policy mandates a drastic reduction in NO_x emissions from diesel engines [1]. To meet this challenge, multiple technical options are being explored, one such example being the NO_x storage/reduction (NSR) catalysis. This system works in a cyclic manner [2], the NO_x in the lean exhaust gas is first stored on the catalyst as nitrates. When the extent of NO_x storage reaches a certain saturation level, the exhaust is deliberately made rich to release the trapped NO_x and reduce it to N_2, thereby regenerating the catalyst. For vehicular applications, the trapping or lean-phase is typically 60–90 s long, while the regeneration or the rich-phase is of the order of 3–5 s. NSR catalysts are typically composed of a basic component, such as Ba or K, to trap the NO_x and precious-metal component, such as Pt, for its redox properties. On a commercial system, the efficiency in transforming the emitted NO_x to N_2 is over 95%. This is remarkable, as the Pt itself is selective for the formation of N_2 from NO and H_2 only in a narrow range of NO to H_2 ratio, as reported in literature [3–5]. A more detailed account of this technology can be found in a recent review [2].

The regeneration step is much less understood than the storage step and only a few studies have addressed the NO_x reduction process. Kabin et al. [6] proposed that the NO_x is released as a result of the heat generated by the exothermic reactions upon switching to the regenerating gases (thermal release), while others have proposed a decrease in the equilibrium stability of the stored nitrates due to either the decrease in the partial pressure of oxygen [7,8], or other compositional changes such as the presence of CO_2 [7,9], or the establishment of a net reducing environment [8,10]. However, Castoldi et al. [11] found that the reduction of stored nitrates does not involve thermal decomposition of the adsorbed NO_x species as a preliminary step. Several routes have been

* Corresponding author. Tel.: +1 765 494 7799; fax: +1 765 494 0805.
E-mail address: fabio@purdue.edu (F.H. Ribeiro).

0920-5861/$ – see front matter
doi:10.1016/j.cattod.2008.01.007

suggested for reduction. Burch and Millington [12] proposed a mechanism in which NO is decomposed on reduced Pt sites, and the role of the reductant is to reduce the oxidized Pt to Pt^0, which is capable of reducing NO to N_2. On the other hand, direct reaction between released NO_x species and the reductant molecules on the precious metal has also been proposed [13]. In addition, reduction by spillover routes has also been proposed. For example, Liu and Anderson [8] have proposed a different mechanism of NO_x release in which the reductant molecule (or its activated form spilled over from Pt) may interact directly with the stored NO_x on the storage component where the nitrates are reduced to nitrites which then release NO and gaseous oxygen. Nova et al. [11,14,15] reported a similar mechanism that involves the activation of H_2 on Pt sites, followed by spillover on the alumina support towards nitrate adspecies that decompose to gaseous NO_x, which is then reduced on Pt or is directly reduced by spilled over hydrogen. They also included the possibility of a mechanism involving surface diffusion of NO_x adspecies toward reduced Pt sites, which reduce the NO_x to N_2. This latter possibility, the reverse spillover of NO_x to the metal and reaction to form N_2 has been suggested by Cant et al. [16] also, but the spillover of hydrogen atoms from metal to BaO was not ruled out either. Other studies involve comparison of different reductants. Abdulhamid et al. [17,18] compared CO, H_2, C_3H_6 and C_3H_8 for the reduction of stored NO_x on a BaO-containing trap catalyst with Pt, Pd or Rh as the precious metal component. They found that H_2 and CO have a relatively high NO_x reduction efficiency compared to C_3H_6 and C_3H_8, and that the Pt and Rh systems also suppressed NH_3 formation at lower temperature (250 °C). Szailer et al. [19] studied nitrate reduction using CO and H_2 on Pt/Al_2O_3 and $Pt/BaO/Al_2O_3$ catalysts and found H_2 to be a more effective reducing agent than CO, with reduction in H_2 occurring at temperatures as low as 150 °C. Similar results were seen by others as well [10,20]. In a recent study, Pihl et al. [21] proposed a schematic of the regeneration process to explain the trends observed during the transient lean–rich cycles involving a reductant front with representative reactions to account for the formation of the byproducts, NH_3 and N_2O, along with N_2 from the stored NO_x, based on the local NO_x-to-reductant ratio in the front, similar to the model we proposed earlier [5].

This paper, which is a continuation of our previous work [5], provides further insights into the mechanism governing the reduction of stored NO_x species on a $Pt/BaO/Al_2O_3$ catalyst when H_2 is employed as a reductant. The objective of the present investigation is to expand our previous study to incorporate the effects of temperature and other exhaust gas components such as CO_2 and H_2O on the regeneration steps. We will show that the reduction process can be explained by the release of NO or NO_2 which is then optimally reduced to N_2 or over-reduced to NH_3 on the Pt clusters. Most importantly, we will provide a model of the reduction process with H_2 reductant that involves NH_3 formation as an intermediate and is as effective as H_2 in reducing stored NO_x. Thus, NH_3 serves as a carrier of H-atoms and is eventually transformed to N_2, maintaining the high selectivity of the trap towards N_2.

2. Experimental methods

The Pt/Al_2O_3 and $Pt/BaO/Al_2O_3$ catalysts used in this study were supplied by EmeraChem, LLC in monolithic form. Both monoliths had a cell density of 200 channels $in.^{-2}$. The Pt loading for both samples was *ca.* 50 g ft^{-3} of monolith. The Ba loading in the washcoat of the $Pt/BaO/Al_2O_3$ sample was 20 wt%. The percentage of metal exposed (PME) or metal dispersion, defined as the ratio of the number of surface Pt atoms to the total number of Pt atoms, measured by H_2–O_2 titration [22], was 42% for the Pt/Al_2O_3 monolith while it was 60% for the Ba-containing catalyst. This gives an exposed Pt content of 6.2 and 8.2 μmol g^{-1} for the Pt/Al_2O_3 and $Pt/BaO/Al_2O_3$ samples, respectively. The Pt/Al_2O_3 sample was 1 in. long, weighed about 3 g and had a cross-section of 60 channels. The total gas flow rate over this sample was 6.6 L min^{-1}, corresponding to a gas hourly space velocity of 80,500 h^{-1}. The $Pt/BaO/Al_2O_3$ catalyst was a 3 in. long core, also with a cross-section of 60 cells. The total flow rate over this sample was 7.0 L min^{-1} corresponding to a space velocity of 30,000 h^{-1}.

The experimental apparatus used for this study is described in detail elsewhere [23] and briefly here. All the experiments reported here were run at 300 °C, except where specified. The NO, NO_2, N_2O, NH_3, CO_2 and H_2O concentrations in the outlet gas stream were detected with an FTIR gas analyzer (MKS MultiGas™ Analyzer, Model 2030), while the N_2 concentration was detected with a quadrupole mass spectrometer (SRS RGA 200). The frequency of data collection was 1 Hz for both the FTIR analyzer and the mass spectrometer. The mass spectrometer was calibrated to measure N_2 concentrations in the 0–6500 ppm range either by the injection of pulses of known volumes of N_2 or by sampling calibrated N_2/Ar mixtures. Argon was used as the carrier gas to allow for the measurement of the released N_2. Mass flow controllers were used to control all the gas flows except for the experiments where high concentrations (>1000 ppm) of NH_3 and NO were utilized. These flows were controlled through needle valves. The system was automated to switch 3-way valves between lean–rich cycles. K-type thermocouples were placed 6 mm before and after the catalyst sample to verify inlet and outlet gas temperatures. To minimize temperature gradients, the inlet gas was preheated before entering the reactor. In the experiments involving water in the feed gas, deionized water was metered by a water pump (Fluid Metering, Inc., Model QVG50). All the gas lines were heated to 120–150 °C. To avoid fluctuations in the water partial pressure, a 1.6 mm (0.0625 in.) diameter tube capillary with an internal diameter of 0.254 mm was used to deliver a continuous flow of water after the gas mixture passed through the pre-heater.

3. Results and discussion

Fig. 1 shows the evolution of the outlet gas concentrations from a $Pt/BaO/Al_2O_3$ catalyst after the switch to the regeneration gases containing 0.75% H_2/Ar at 300 °C, adapted from our previous work [5]. The regeneration or rich-phase was preceded by a 7 min long trapping or lean-phase, with

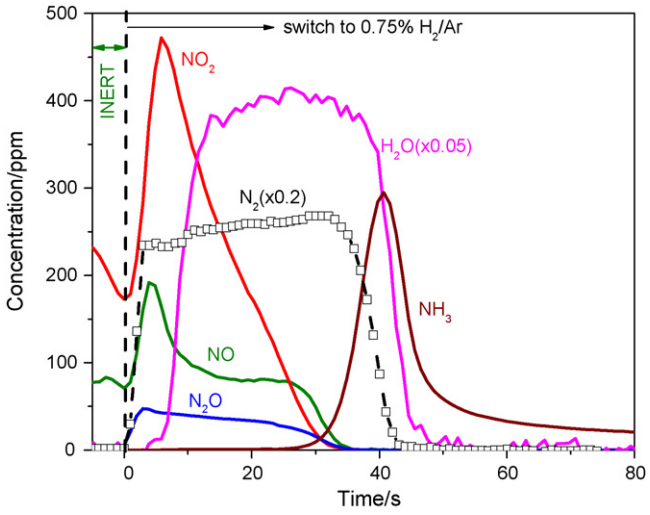

Fig. 1. Typical concentration profiles during regeneration of the $Pt/BaO/Al_2O_3$ catalyst with 0.75% H_2/Ar at 300 °C, 30,000 h^{-1} SV, adapted from our previous work [5]. The regeneration phase is preceded by a 7 min capture/lean-phase with 350 ppm NO, 10% O_2, balance Ar and a 5 s purge with Ar at 300 °C. Data reprinted from reference [5], © 2006, with permission from Elsevier.

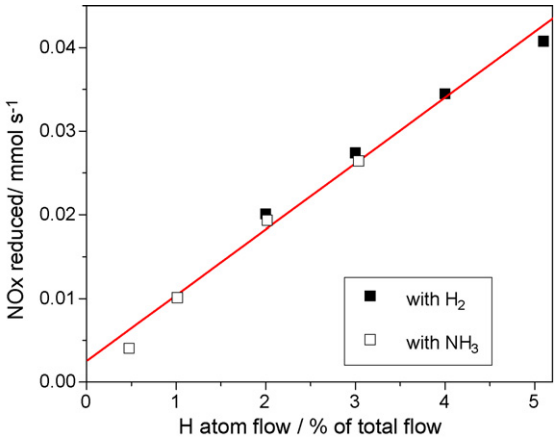

Fig. 2. Overall rate of NO_x reduction (moles of NO_x reduced divided by the time to regenerate completely) as a function of rate of flow of H-atoms in the form of H_2 or NH_3 at 300 °C. Time required to regenerate the trap catalyst is measured by the width of the N_2 pulse in the mass spectrometer. The H-atom flow rate is expressed as a percentage of total flow rate.

composition 350 ppm NO, 10% O_2, balance Ar, and a 5 s purge with Ar. The catalyst reached 93% of the NO_x saturation amount during the 7 min of storage. Although the rich gases were passed over the NO_x saturated catalyst for about 3 min, the catalyst was completely regenerated in about 50 s for the corresponding 7 min of NO_x storage, as can be seen in Fig. 1 from the width of the N_2 and H_2O traces, the two main regeneration products. The selectivity of the total stored NO_x for the formation of N_2 was about 85%. To obtain reproducible results, it was necessary to run 4–5 lean–rich cycles. The nitrogen balance between capture and regeneration phases was found to close within experimental error; for the NO_x storage of 0.53 mmol during the 7 min lean period, the total amount of N-based species (N_2, NH_3, N_2O, NO_2, NO) in the rich period was 0.52 mmol, with N_2 measurements made using the quadruple mass spectrometer, while the other N-species quantified by the FT-IR gas analyzer, as noted in the experimental methods. After the regeneration phase, the same amount of NO_x was stored (0.53 mmol) during the subsequent 7 min capture phase. Similar concentration profiles, as noted in Fig. 1, have also been reported by Nova et al. [24] and Pihl et al. [21].

As seen in Fig. 1, both the N_2 and H_2O traces increase rapidly to a constant value until the end when they sharply decrease. This rectangular wave shape indicates a ''plug flow'' type of mechanism implying a complete reaction between the reductant H_2 and the NO_x to produce N_2 and H_2O. The H_2 signal was measurable only close to the end of the cycle, suggesting that the reductant is the limiting reactant in the regeneration phase. The H_2 gets consumed to below detection level during the regeneration process and slips only when the stored NO_x starts to deplete towards the end of the catalyst bed. The H_2 data are not shown in Fig. 1, since only non-quantifiably small H_2 amounts were observed in the mass spectrometer before breakthrough, and the H_2 concentration measurement was not precise. Since the reductant is the limiting reagent, this implies that the time for regeneration (as indicated by the width of the near rectangular N_2 pulse or equivalently, the breakthrough time of H_2) should be inversely proportional to the reductant amount fed per unit time, for the same amount of NO_x reduced. To verify this, experiments were performed by varying the H_2 flow rate in the regenerating phase over the range of 70–175 sccm at the same space velocity (30,000 h^{-1}, total flow of 7000 sccm, balance Ar) on the $Pt/BaO/Al_2O_3$ catalyst. In all cases, the evolution of H_2 (observed in the mass spectrometer) was delayed, indicating that the reductant was completely consumed during the initial stages of the regeneration phase. The results are shown in Fig. 2, where the ordinate represents an overall rate of NO_x reduction, *i.e.*, the total moles of NO_x reduced divided by the time needed to regenerate the trap catalyst completely, while the abscissa represents the rate at which H-atoms (in the form of H_2 in this case) are introduced, expressed as a percentage of the total flow rate (constant, *ca.* 7000 sccm). The linear relationship shows that the time required for complete regeneration is inversely proportional to H_2 flow, for a given amount of NO_x to be reduced, thereby confirming that the supply of hydrogen is limiting. The selectivity to N_2 was maintained at 80–85% in these experiments. Nova et al. [24] had also noticed that the N_2 production during the regeneration of a $Pt/BaO/Al_2O_3$ catalyst is limited by the amount of H_2 fed to the reactor. Likewise, increasing the H_2 supply rate by increasing the space velocity at a fixed H_2 concentration is expected to have an identical linear effect on the overall rate of NO_x reduction.

We also observed (Fig. 3) that lowering the temperature for the tests to 250 °C, or even 200 °C, at a given H_2 flow made no difference on the reduction profiles or the time scales of the regeneration. More N_2O, nearly twice the amount produced at 300 °C, was produced at these lower temperatures, although it was still negligible to the other N-based products, as will be discussed later. Pihl et al. [21] also found the N_2O formation to increase at lower temperatures. Moreover, incorporating other exhaust gas components such as CO_2 and H_2O in the feed also

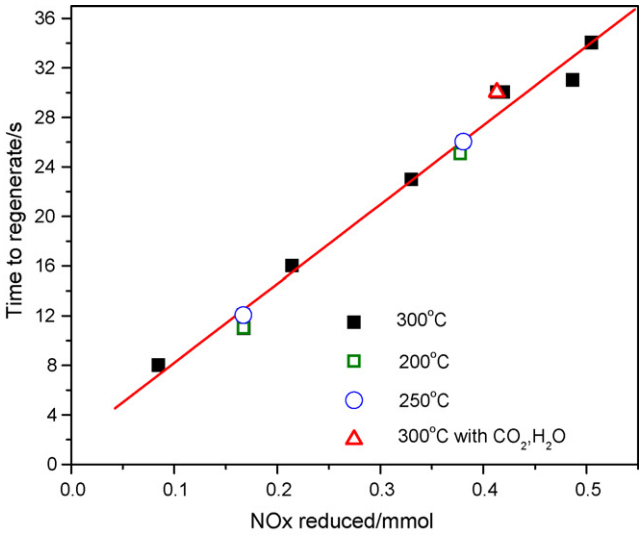

Fig. 3. Time to regenerate the trap catalyst at different levels of NO_x saturation using 1% H_2/Ar at different temperatures and gas compositions.

had no effect on the regeneration time. This is shown in Fig. 3, where the time required to completely regenerate the catalyst (as measured by the width of the effluent N_2 pulse, or from the H_2 breakthrough time) is presented as a function of the NO_x reduced, for a constant H_2 flow corresponding to a H_2 concentration of 1% in Ar. As can be seen, the results obtained at 200 and 250 °C, and also those with 8% CO_2 and 8% H_2O in the feed at 300 °C fall on the same linear curve (the slope of which is the reciprocal of the overall rate of NO_x reduction) obtained at 300 °C in the absence of CO_2 and H_2O. Thus, the reduction rate is not affected by the temperature (in the 200–300 °C range) or by the presence of CO_2 and H_2O (tested only at 300 °C) and is governed only by the supply of the reductant H_2, which was fixed in these experiments. Note that some H_2 consumption will be seen even in the absence of stored NO_x due to the reduction of the exposed Pt on the catalyst that has been oxidized in the previous lean-phase. The linear trend shows H_2 consumption for about 3 s (*Y*-intercept) in the absence of stored NO_x, in good agreement with the calculated H_2 consumption for 3.1 s for the reduction of the 0.074 mmol of the exposed platinum on this catalyst from PtO_2 to Pt. This observed insensitivity in the reduction rate to both, temperature and gas composition suggests that the regeneration is not limited by the kinetics but by the supply of the reductant as noted earlier. Note that at sufficiently lower temperatures (<200 °C), the reaction kinetics may not be able to keep up with the reductant supply rate and may become limiting.

To check this limitation imposed by the stoichiometric supply of the reductant required to reduce the stored NO_x, the rate of supply of H_2 was compared with the experimentally measured overall rate of NO_x reduction and also to the external mass transfer rate. Mass transfer to the tube walls was described through the use of a mass transfer coefficient (k_m), which is related to the Sherwood number (*Sh*):

$$Sh = \frac{k_m d_p}{D_g} \quad (1)$$

where k_m is the mass transfer coefficient, d_p is the diameter of the monolith channel, and D_g is the gas phase diffusivity. The Sherwood number was estimated through the use of the correlation given by Hayes and Kolaczkowski [25] for laminar flow in a monolithic channel with reaction at the wall. The correlation gives an average value for the Sherwood number over the entire reactor length and is given by:

$$Sh = 3.66\left\{1 + 0.095\frac{d_p}{L}Pe_M\right\}^{0.45}$$
$$Pe_M = \frac{u d_p}{D_g} \quad (2)$$

where L is the reactor length, Pe_M is the Peclet mass transfer number, and u is the gas phase velocity. Using these correlations, the value of mass transfer coefficient obtained under our flow condition is 0.5 m s^{-1}. The maximum rate of mass transfer of the reductant H_2 to the tube wall, given by $k_m \underline{a} [H_2]_g$, with $\underline{a}$ as the specific interfacial area (*ca.* 2230 m^{-1} for our monolithic catalyst), is calculated to be 9.3×10^{-4} mol cc^{-1} s^{-1} for a gas phase H_2 concentration ($[H_2]_g$) corresponding to 2% in Ar. As against this, Fig. 2 indicates that at 2% H_2/Ar (or H-atom flow of 4% of the total flow), the overall rate of NO_x reduction is 3.4×10^{-5} mol s^{-1}, or the corresponding volumetric rate is 2.5×10^{-6} mol cc^{-1} s^{-1}. This is about 380 times lower than the mass transfer rate calculated above at the same H_2 flow. Moreover, the measured overall rate is comparable to the rate of supply of H_2 to the catalyst, calculated to be 6.8×10^{-6} mol cc^{-1} s^{-1} for a 2% flow of H_2 in Ar at a total flow of *ca.* 7000 sccm and normalized by the total catalyst volume. This H_2 supply rate is about 2.8 times higher than the measured NO_x reduction rate, close to the stoichiometric H_2 requirement of 2.5 to reduce a nitrate molecule to N_2, as per the overall reaction:

$$NO_3^- + 2.5H_2 \rightarrow OH^- + 2H_2O + 0.5N_2 \quad (3)$$

These observations confirm that the process is not mass transfer or kinetically limited, but is controlled by the supply of the reductant H_2.

Fig. 4 shows the selectivity of the NO_x reduction over the Pt/BaO/Al_2O_3 trap catalyst towards N_2, measured on an N-basis, as a function of the NO_x stored in the previous lean cycle. The NO_x storage amount was varied by using different NO_x adsorption time lengths (1–7 min) with the same feed containing 350 ppm NO, 10% O_2, balance Ar at 300 °C and 30,000 h^{-1} space velocity. The regeneration feed contained 2% H_2/Ar. Fig. 4A shows that the regeneration was complete, since all the NO_x stored in the capture phase could be accounted for by the N-species seen in the regeneration phase (N_2, NH_3, N_2O, NO_2, NO) as is evidenced by the nitrogen material balance (the 45° black line in Fig. 4A), which closed to within 10%, relative to stored NO_x. Moreover, the N_2 selectivity was highest (about 96%) for the typical cycle time of 60 s lean–6 s rich, and decreased for longer NO_x storage duration, as more byproducts like NH_3 or N_2O were formed (Fig. 4B). Similar results were also reported by Nova et al. [24] with N_2 selectivity increasing with decreasing NO_x loading in the temperature range 250–350 °C. Abul-Milh and Westberg [26] also found that the

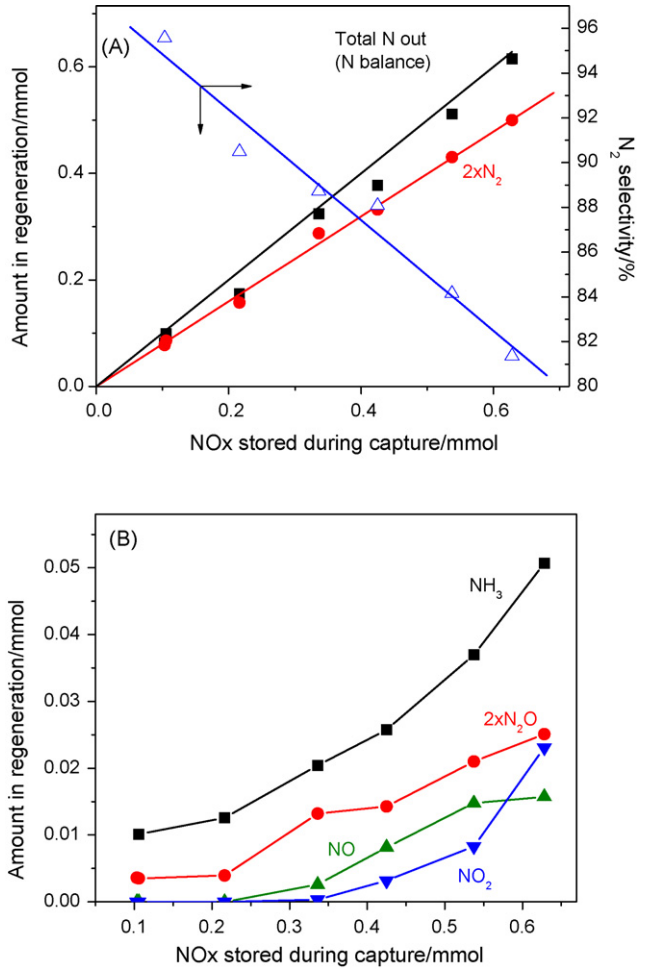

Fig. 4. Amounts of N-species observed during regeneration phase as a function of NO_x stored during the previous capture phase at 300 °C. Feed for capture: 350 ppm NO, 10% O_2, balance Ar. The capture time was varied from 1 to 7 min. Feed for regeneration: 2% H_2/Ar. (A) Total N-species (N material balance shown by the black 45° line), N_2 and N_2 selectivity on N basis, (B) NH_3, N_2O, NO and NO_2. The curves are shown for visual guidance.

formation of NH_3 increases with increasing amount of stored NO_x, as we found in Fig. 4B. The high N_2 selectivity shown in Fig. 4A for the Pt/BaO/Al_2O_3 catalyst is remarkable, since Pt itself is selective for the formation of N_2 from NO and H_2 only in a narrow range of NO to H_2 ratio, as has been reported in literature [3,4,21] and as we also found in our experiments with Pt/Al_2O_3 catalyst without the storage component, discussed next. We investigated the reaction of H_2 with NO over a Pt/Al_2O_3 catalyst as a way to simulate the reduction step. The Pt/Al_2O_3 monolith catalyst was first exposed to about 0.5% NO/Ar mixture for 2 min and then H_2 was added to the NO flow at varying NO:H_2 ratios for 6 min. The reactions reached steady state in less than 1 min. Table 1 shows the steady-state reactant conversion and product selectivity at 300 °C as a function of NO:H_2 ratio in the feed. The NO:H_2 ratio was varied to simulate the different NO_x/reductant environments that occur along the NSR trap. The data reported was obtained by averaging the concentrations after 2 min of reaction.

As seen in Table 1, when all the reduction chemistry occurs on Pt, then the steady-state selectivity to N_2 is a strong function

Table 1
Steady-state product selectivity and reactant conversion at 300 °C as a function of NO to H_2 ratio in the feed for the reaction of NO + H_2 over a Pt/Al_2O_3 monolith

NO:H_2	Conversion (%)		Selectivity		
	NO	H_2	NH_3	N_2	N_2O
0.40	99.7	67.3	0.77	0.23	0.00
0.54	99.7	82.0	0.41	0.58	0.01
0.92	99.7	100	0.10	0.89	0.01
1.74	70.5	100	0.00	0.65	0.35
4.60	43.4	100	0.00	0.36	0.64

Feed contains *ca.* 0.5% NO, 0.12–1.2% H_2, balance Ar.

of the NO:H_2 ratio. The H_2 conversions noted in Table 1 were calculated based on the amounts of N_2, NH_3 and N_2O formed and the appropriate reaction stoichiometry, since the H_2 concentration was not measured precisely (as also noted earlier). The selectivity to N_2 is defined as the ratio of two times the total amount of N_2 formed to the total amount of nitrogen species in the product (N_2O, NH_3, and N_2) formed during the reaction on an atomic N basis. Table 1 shows that as the NO:H_2 ratio increases from 0.4 (excess H_2) to 4.6 (excess NO), the product selectivity changes from mostly NH_3 at low NO:H_2 ratios to N_2O at high NO:H_2 ratios. The highest N_2 selectivity was observed around a stoichiometric ratio (1:1) of NO:H_2. The formation of mostly NH_3 under low NO:H_2 ratios (reducing conditions) has previously been observed by Shelef et al. [27] and also recently by Lindholm et al. [28] and Pihl et al. [21], the latter results obtained on a commercial NSR catalyst assuming no NO_x is stored on the trap catalyst under net reducing conditions. The product selectivities we have obtained for the NO + H_2 reaction over the Pt/Al_2O_3 monolithic sample are similar to that reported by Kosaki et al. [3] for their Pt/Al_2O_3 powdered catalyst. Most of the experiments were carried out under nearly isothermal conditions (300 °C). However, in experiments where a significant amount of NH_3 was formed (low NO:H_2 ratio), the outlet gas temperature was 30–40 °C higher than that of the inlet. For this reason, we carried out experiments at 200 °C to make sure the selectivity trend seen was not due to a hot spot. We observed similar product selectivity to that at 300 °C. Based on our trap regeneration model which involves a moving front of the reductant H_2, the concentration of H_2 will be high at the beginning of the front, and hence the NH_3 selectivity at the beginning of the front should be high as seen in the above NO + H_2 experiments on Pt/Al_2O_3. However, Fig. 4 shows poor selectivity towards NH_3 on the trap catalyst, with majority of the stored NO_x being reduced to N_2 by H_2.

To further investigate the contradictory behavior of the two Pt catalysts (with and without Ba) during NO_x reduction, NH_3 was tested as a reductant for both catalysts. Table 2 shows the results of the experiments with NO + NH_3 on the Pt/Al_2O_3 catalyst, similar to the NO + H_2 experiments described above. Analogous to the NO + H_2 reactions (Table 1), the selectivity of the NO + NH_3 reactions is also a function of the ratio of the reactants in the feed. As the NO:NH_3 ratio was varied from 0.67 (excess NH_3) to 5 (excess NO), the product selectivity changed

Table 2
Steady-state product selectivity and reactant conversion at 300 °C as a function of NO to NH_3 ratio in the feed for the reaction of NO + NH_3 over a Pt/Al_2O_3 monolith

NO:NH_3	Conversion (%)		Selectivity	
	NO	NH_3	N_2	N_2O
0.67	99.6	51.2	0.99	0.01
1.00	99.6	63.1	0.99	0.01
1.33	99.6	78.4	0.99	0.01
2.00	97.3	99.5	0.74	0.26
5.00	55.6	98.2	0.36	0.64

Feed contains *ca.* 0.45% NO, 0.09–0.68% NH_3, balance Ar.

from mostly N_2 at low NO:NH_3 ratios to N_2O at high NO:NH_3 ratios. Otto et al. [29] have previously shown that NH_3 is an effective reductant in the removal of NO from waste effluents over supported Pt. The formation of N_2 as the sole product under equimolar NO:NH_3 condition at 300 °C has also been reported by Pihl et al. [21]. We have also carried out experiments involving N_2O and H_2 at 300 °C over the Pt/Al_2O_3 catalyst. In this case, with about 50 ppm N_2O and 1% H_2 at 300 °C, the N_2O was reduced to N_2 and H_2O at a total

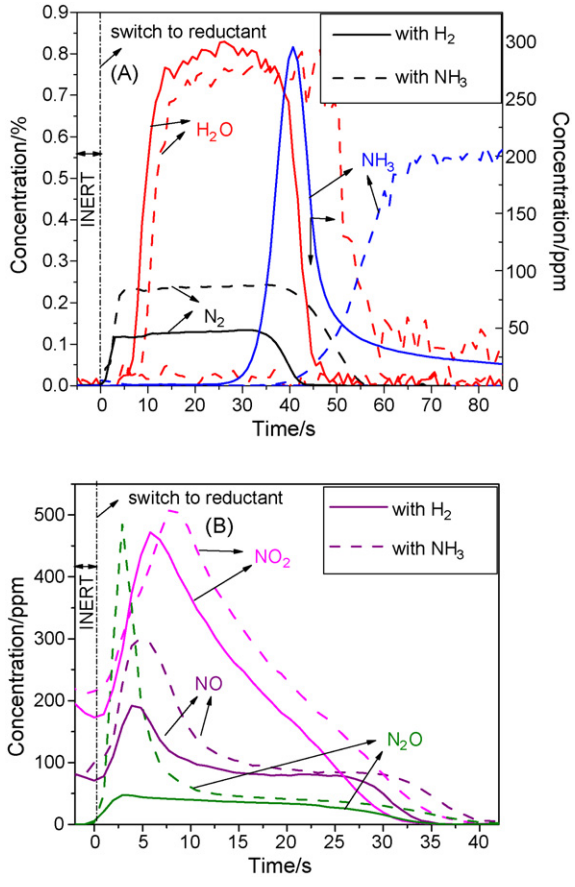

Fig. 5. Evolution of the species after the switch to the regeneration phase following a 7-min trapping period with 350 ppm NO/10% O_2/Ar at 300 °C over a Pt/BaO/Al_2O_3 monolith, adapted from our previous work [5]. The solid lines represent regeneration with 0.75% H_2/Ar and the dashed lines represent regeneration with 0.53% NH_3/Ar. The space velocity over the catalyst is 30,000 h^{-1}. (A) N_2, H_2O and NH_3 traces, (B) NO_2, NO and N_2O traces. Reprinted from reference [5], © 2006, with permission from Elsevier.

conversion of 90%. The results for NO reduction with H_2 or NH_3 show that selectivity to N_2 is high only in specific ranges of oxidant to reductant ratios; low NO:H_2 ratios, as may be expected during the beginning of the reductant front, favor NH_3 formation, while low NO:NH_3 ratios show high N_2 selectivity. It also shows that the selectivity for NH_3 or H_2 as reductants is similar.

In addition to the above NO + NH_3 reactions on the Pt/Al_2O_3 catalyst, we also used NH_3 for regenerating a Pt/BaO/Al_2O_3 trap catalyst and compared the results with the regeneration with H_2. Fig. 5 shows a comparison of the evolution of the outlet gas concentrations from a Pt/BaO/Al_2O_3 catalyst after the switch to regeneration gases containing either H_2 or NH_3 at 300 °C, adapted from our previous work [5]. The solid lines indicate regeneration with 0.75% H_2/Ar, and are the same as those shown in Fig. 1, while the dashed lines indicate regeneration with 0.53% NH_3/Ar. The number of hydrogen atoms per unit of time flowing over the sample in the regenerating gas mixture was kept nearly identical in both cases to illustrate the effectiveness of H_2 and NH_3 for regeneration. Similar to the experiment shown in Fig. 1, the regeneration phase shown in Fig. 5 also followed a 7 min long trapping (lean) phase that contained 350 ppm NO, 10% O_2, balance Ar, and a 5 s purge with Ar.

As seen in Fig. 5A, at 300 °C, the N_2 and H_2O traces during regeneration with NH_3 have the same rectangular wave shape as those seen with H_2. Like H_2, NH_3 was also found to get completely consumed during the regeneration process and slipped only at the end of the bed when the stored NO_x was depleted, making it the limiting reactant. The regeneration in NH_3, thus, shows the characteristic "S" shaped curve for NH_3 evolution, representative of strong gas adsorption seen, for example, during adsorption of NO_2 on BaO. This NH_3 breakthrough is similar to the model presented by Epling et al. [30] for NO_x storage, where the NO_x sorption zone propagates down the catalyst bed in a plug flow manner and begins to breakthrough after reaching the end of the catalyst bed. Thus, the NH_3 trace seen during regeneration in NH_3 is consistent with our plug flow model. Fig. 5A also shows that the H_2O and N_2 traces in the case of NH_3 as the reductant continue at constant levels for a 15% longer duration before starting to decrease, when compared to the case with H_2 as the reductant. This difference is caused by the uncertainty in the reproducibility of the total flow rate. The H_2O trace when NH_3 is used as a reductant did not return to the zero level because of the presence of H_2O as an impurity in the NH_3/Ar gas mixture used. If one accounts for this H_2O impurity, the area under the H_2O traces of Fig. 5A for the two reductants are similar within error (*ca.* 1.39 and 1.31 mmol). More N_2 is produced when NH_3 is used as the reductant (0.74 mmol vs. 0.22 mmol) since, in addition to the nitrogen species in the stored NO_x, NH_3 also contributes to the total N_2 formed through its oxidation by the NO_x and may also contribute additional NO_x species by reaction with oxygen.

To summarize the findings, NH_3 is capable of regenerating the trap in a similar way as H_2. In fact, NH_3 was found to be as effective as H_2 in the regeneration process. This is evidenced in

Fig. 2, described earlier with H_2 as the reductant. The results obtained with NH_3 as the reductant at the same temperature (300 °C) were found to lie on the same straight line obtained earlier with H_2. This further corroborates the fact that the regeneration process is limited only by the supply of H-atoms required to reduce all the stored NO_x, and also indicates that the trap catalyst does not differentiate between the source of the H-atoms, H_2 or NH_3. This insensitivity towards the reductant type confirms the equivalency between NH_3 and H_2 and also supports the coupling of catalytic and stoichiometric kinetics during the regeneration process, as discussed before.

Based on these results on Pt/Al_2O_3 and $Pt/BaO/Al_2O_3$ using H_2 or NH_3 as reductants, we propose NH_3 as an intermediate species formed within the reductant front during the regeneration of the trap catalyst with H_2 by the reaction between the stored NO_x and H_2. Fig. 6 shows a schematic of the proposed regeneration mechanism for a single monolith channel of a $Pt/BaO/Al_2O_3$ NSR catalyst. The figure illustrates the propagation of the reductant front along the catalyst bed with complete regeneration of the trapping sites. It shows that as the NO_x ($NO + NO_2$) is released from the trapping sites (the exact mechanism of release is not known), it reacts with H_2 over Pt to form NH_3, N_2 and N_2O as the N-containing species. The selectivity of the individual species will depend on the local NO_x:H_2 concentration ratios as shown in Table 1. In the beginning of the front, where the H_2 level is high compared to the NO_x, the reaction with the released NO_x over Pt will form mostly NH_3 and some N_2, based on Table 1. The NH_3 formed, however, will not slip out of the catalyst, but instead it will further react with more NO_x to give either N_2 or N_2O, based on Table 2. If the N_2O is formed behind the front, it will be reduced to N_2 by H_2 or NH_3. The N_2O concentration profile observed and an alternate route of N_2O formation is further discussed below. As the front approaches the end of the catalyst (lower panel of Fig. 6), the supply of NO_x starts to deplete and will be insufficient to react with the NH_3 formed upstream, leading to the NH_3 breakthrough seen in Fig. 1 or Fig. 5A with H_2 reductant. Before the reaction front reaches the end of the bed, most of the non-selective products formed by the reaction of H_2 with NO_x over Pt, such as N_2O and NH_3, will further react to form N_2 and maintain the high N_2 selectivity of the overall NSR catalyst, as seen in Fig. 4A. Using this rationale, and by reference to Table 1, one might expect that as the concentration of H_2 is depleted at the end of the reductant front, N_2O should become a major product. This is not observed experimentally. We believe the reason is that there is a self-adjusting mechanism. As the concentration of H_2 is lowered, the amount of released NO is also apparently lowered thus keeping the local overall NO:H_2 ratio unfavorable to the formation of N_2O. As can be seen from Fig. 4B, the N_2O amounts formed are very small (5×10^{-3} mmol with H_2, 0.014 mmol with NH_3), even less than the amount of Pt exposed on the catalyst (0.074 mmol). We hypothesize that this N_2O is formed in a stoichiometric reaction between Pt and NO giving N_2O and Pt-O and is confined only to the leading edge of the reductant front where the H_2 gets depleted creating a non-reducing environment. In particular, we have observed that the reaction between NO and reduced Pt in the absence of adsorbed hydrogen will produce N_2O until the surface is titrated to Pt-O and the reaction stops. This is consistent with the N_2O and NO traces in Fig. 5B. The traces were found to be similar for both H_2 and NH_3 reductants except for a higher initial spike when NH_3 is used. The near constant concentration of NO and N_2O (after the spike) with time is an indication of they escaping from the reduction front (particularly the leading edge, as discussed above). Lietti et al. [31] also observed N_2O amounts smaller than the exposed Pt to be produced during the regeneration of the stored NO_x on $Pt/Ba/Al_2O_3$ using H_2 at 200 °C. However, they attributed its formation to be from the direct reaction between barium nitrate/nitrite and H_2.

Thus, the shape of the NH_3 evolution curves for the H_2 and NH_3 cases are consistent with our plug flow model. In the case of regeneration by H_2, the NH_3 evolution curve is the result of the competition between its generation by $NO_x + H_2$ reaction and its subsequent consumption by the stored NO_x. The reason NH_3 is seen only towards the end of the cycle is due to the fact that the NH_3 formed in the front gets completely consumed in reducing the NO_x to N_2 as the front moves along the length of

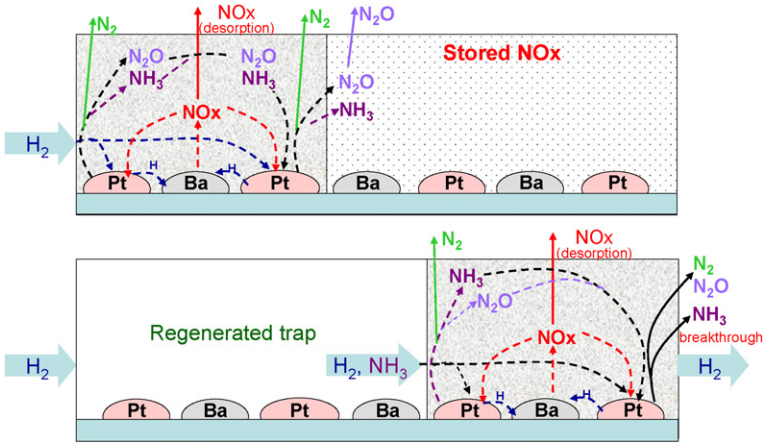

Fig. 6. Depiction of the reduction mechanism for a $Pt/BaO/Al_2O_3$ monolith regenerated with H_2. The upper panel shows the propagation of the reductant front along the catalyst length, producing N_2 as the main product while the lower panel illustrates the process when the front reaches breakthrough, releasing NH_3 as the major product.

the catalyst. Only when the NH_3 front reaches the end of the catalyst bed, it begins to break through due to the absence of NO_x to oxidize the NH_3 to N_2 and H_2O. Thus, NH_3 forms *in situ* during regeneration with H_2 and serves as a carrier of H-atoms. In fact, if the regeneration phase in H_2 is not allowed to go to completion by decreasing the time of rich pulse, so that NO_x stays accumulated on the catalyst, insignificant NH_3 formation is seen in the rich-phase, consistent with our model. For example, following a 7 min NO_x storage phase with 350 ppm NO, 10% O_2, balance Ar, it takes about 20 s to regenerate the catalyst completely with 2% H_2/Ar at 300 °C, with significant NH_3 formation seen (NH_3 maxima about 800 ppm), similar to the results shown in Fig. 1. However, when the rich-phase is limited to only 5 s under similar conditions of NO_x storage and regeneration, so that the NO_x stays accumulated at the end of the rich pulse, the corresponding NH_3 maxima seen is only about 1 ppm (results not shown), since the NH_3 formed *in situ* gets completely consumed in reducing the NO_x in that 5-s pulse, without breaking through.

According to Nova et al. [24], the delayed NH_3 formation seen after the N_2 production, nearly coincident with the H_2 breakthrough is related to the reduction of nitrate species stored on Ba sites far from Pt and/or to a high H/N ratio on the catalyst surface. However, in light of the plug flow mechanism we have proposed, a high H/N ratio will be prevalent at the beginning of the regeneration front and this should result in significant NH_3 formation all along the catalyst bed as the front progresses. This is inconsistent with the experimentally seen NH_3 peak only at the end of the regeneration cycles, which can only be explained by the involvement of NH_3 in the regeneration process in the form of an intermediate, as we have proposed. Recently, Pihl et al. [21] also suggested a similar plug-flow model for the trap regeneration. In this case, the delayed NH_3 appearance was postulated to be due to its formation from the NO_x released from the "slow NO_x release sites" upstream of the reduction front, a zone with high reductant concentration. Any NH_3 (formed upstream of the front) that slips past the front will get oxidized (to N_2 or N_2O) by the NO_x or O_2 stored downstream of the front and hence will not appear in the catalyst effluent until the entire catalyst is reduced/regenerated. However, this explanation would require a secondary, slow formation of NH_3 oxidation products, *viz.* N_2 and N_2O, differentiated from their primary formation from the directly released NO_x, inconsistent with the N_2O trace and the rectangular N_2 trace observed during the regeneration process with H_2 (Fig. 1). The "slow sites" rationale would also suggest a possible role of kinetics in the overall regeneration process, contrary to the results of this study which indicate that the regeneration is not controlled by the kinetics but by the supply of the reductant in the 200–300 °C range as noted earlier. Further, it also cannot explain the equivalency between H_2 and NH_3 in regenerating the catalyst. All these differences make the NH_3 intermediate model proposed in this work more favorable for the trap regeneration process.

The sharp rise in the N_2 trace, as seen in Fig. 5A, implies that the H_2O trace, the other product of the reduction reaction, should follow a similar profile. Although the curve shapes are

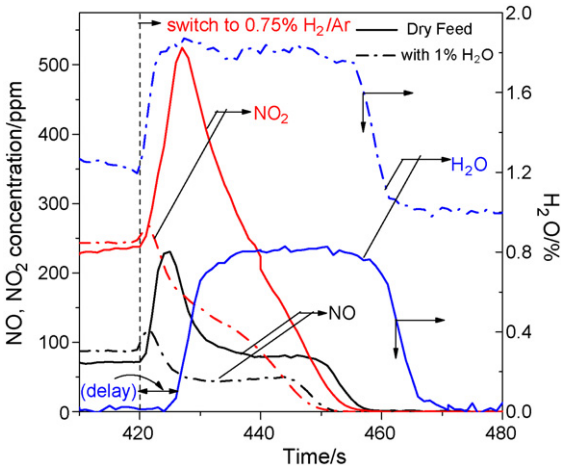

Fig. 7. NO, NO_2 and H_2O concentration profiles obtained during regeneration with 0.75% H_2, 0 or 1% H_2O, balance Ar at 300 °C. The regeneration phase is preceded by a 7 min capture/lean-phase with 350 ppm NO, 10% O_2, 0 or 1% H_2O, balance Ar at 300 °C. The dry feed case clearly shows the delay in the H_2O signal and the concomitant taller NO and NO_2 spikes relative to the wet feed case upon switch to the reductant.

similar, a delay is seen in the H_2O trace, relative to N_2, for both H_2 and NH_3 reductants. We investigated this phenomenon by including H_2O (*ca.* 1%) in both the capture and regeneration phases, the results for which are shown in Fig. 7 with 0.75% H_2/Ar as the reductant. Interestingly, the usual NO_x spike that arises immediately after the switch to the regeneration phase decreased by a factor of two compared to the dry feed conditions, and the H_2O trace had a sharp rise similar to the N_2 trace (*i.e.*, no delay) when H_2O was included in the feed. In light of this data, we propose the following. It is well known that H_2O decreases the NO_x storage capacity of the NSR catalysts [2] and hence H_2O could be competing for some of the NO_x sites. In our case, the NO_x storage decreased from 0.53 mmol under dry conditions to 0.45 mmol in the presence of H_2O. In the absence of H_2O in the trapping or lean-phase, the sites that generally favor the adsorption of H_2O over NO_x (*e.g.*, Al_2O_3) are occupied by NO_x. However, when H_2O is formed during the regeneration phase due to the reductant coming into contact with either residual O_2 or stored NO_x, it first adsorbs on those sites that favor H_2O adsorption over NO_x, causing the delay in H_2O evolution, while displacing the NO_x that were stored on those sites, resulting in a larger NO_x spike. When H_2O is added to the feed during the trapping phase, it is preferentially adsorbed on some of the sites during the capture phase (decreasing the NO_x storage) and this prevents the adsorption of the H_2O that is formed during the regeneration phase, resulting in the sharp rise (no delay) in the H_2O trace and a decreased NO_x spike. However, a small NO_x spike (about 5% of total NO_x stored) is still observed at the beginning of the regeneration phase even in the presence of H_2O in the trapping phase. We hypothesize that this is due to desorption of NO_x upon switch to the regenerating gases (explained below). Note that, even though the NO_x spike at the lean–rich interface under dry feed conditions may be explained by its displacement by the H_2O produced causing the delay in the H_2O signal, a quantitative

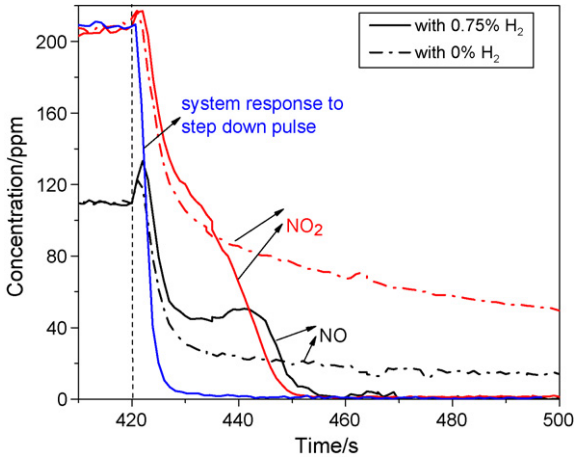

Fig. 8. NO and NO_2 traces upon regeneration with 0 or 0.75% H_2, 8% CO_2, 8% H_2O, balance Ar at 300 °C. The regeneration phase is preceded by a 7 min capture/lean-phase with 350 ppm NO, 10% O_2, 8% CO_2, 8% H_2O, balance Ar at 300 °C. The system's response to a step down pulse of NO is also shown for reference.

match is not possible since the H_2O produced is in percentage scale while the NO_x spike is about 700 ppm under dry feed conditions. Comparing the amounts of H_2O produced and the NO_x present in the spike under the wet and dry fed conditions, we found that per mole of NO_x stored in the previous lean cycle, about 2.3 mol of the water produced was adsorbed, while only 0.05 mol of extra NO_x was seen in the corresponding spike under dry feed conditions in the rich-phase, relative to the wet feed conditions.

The NO_2 trace seen during the regeneration of the trap is proposed to be simply due to the desorption of NO_x arising from the shift in equilibrium between the surface and the gas phase that is accompanied with the switch to the NO_x- and O_2-free regenerating gases and also to the presence of CO_2 and H_2O [8,32]. Fig. 8 shows the NO and the NO_2 effluent concentration profiles during regeneration with 0.75% H_2, 8% CO_2, 8% H_2O, balance Ar at 300 °C. Prior to this regeneration, the catalyst was exposed to the lean gases containing 350 ppm NO, 10% O_2, 8% CO_2, 8% H_2O, balance Ar for 7 min resulting in a NO_x storage of 0.46 mmol. As can be seen from Fig. 8, the decrease in the NO_2 signal is nearly linear with time and is explained as follows. As the catalyst bed is reduced in a plug flow type mechanism, the amount of NO_2 that is available for desorption ahead of the front decreases linearly with time which results in a linear decrease in the NO_2 evolution with time. To reinforce the hypothesis of NO_2 desorption, we performed experiments with an inert substitute (*i.e.*, with no reductant) in the regeneration phase spanning the same regeneration time period (*ca.* 3 min) as with H_2 above. The corresponding NO_x concentration profiles in the absence of H_2 are shown in Fig. 8. No NH_3 or N_2O formation was observed during the regeneration phase in absence of the reductant. After a 7 min trapping phase, storing a similar NO_x amount (0.46 mmol), about 11% of the stored NO_x was found to desorb as NO_2 while only 3% desorbed as NO under the inert flow conditions during the 3 min regeneration period compared to 3% as NO_2, 1.5% as NO under H_2 rich conditions.

The reduction model proposed in Fig. 6 indicates that the trapping phase of the NSR cycle should not extend up to the full capacity of the trap since in that case the NO_x released during regeneration would not be captured downstream, thereby lowering the N_2 selectivity. This is supported by the results shown in Fig. 4A and also by the results of Nova et al. [24], where N_2 selectivity was found to decrease as more NO_x was stored, nearing its full capacity. Furthermore, we propose that having an oxygen storage capacity (OSC) substrate such as ceria could allow the oxidation of NH_3 by the consumption of the H-atoms formed from the dissociation of NH_3 on Pt, leaving N atoms on the Pt surface to recombine and desorb. In that case, the OSC would decrease the NH_3 slip in the NSR catalysts.

4. Conclusion

We have proposed the formation of NH_3 as an intermediate during the regeneration of the $Pt/BaO/Al_2O_3$ lean NO_x trap catalyst when H_2 is used as a reductant. The regeneration process involves the release of NO_x from the trapping site in the gas phase followed by its reduction over Pt, and it may not be necessary to invoke a mechanism of surface-diffusion of the NO-containing species. The process is localized, occurring at the plug flow front of the reductant where it gets completely consumed by the NO_x, forming mostly N_2 and H_2O at the constant rate with which the plug moves along the catalyst length. The chemistry is found to be fast and insensitive to changes in temperature or presence of CO_2 and H_2O, but is limited only by the supply of hydrogen atoms. The catalyst does not differentiate between H_2 or NH_3 as the source of H-atoms, and NH_3 is as effective as H_2 in regenerating the trap catalyst, giving similar concentration profiles of the various species. Despite the narrow NO_x:H_2 ratio window for selective N_2 formation over Pt, the NSR catalyst is capable of converting the NO_x to mostly N_2, because the other products that form over Pt, *viz.* N_2O and NH_3, are either not favored (N_2O) or further react to produce N_2. Thus, NH_3 formed from the reaction between the released NO_x and H_2 continues to react further with the NO_x and gets oxidized to N_2. The NH_3 slip at the end of the rich cycle with H_2 occurs as a result of the reductant front reaching breakthrough where the NO_x left is insufficient to consume the NH_3 formed. The low observed amount of N_2O is consistent with its formation in a stoichiometric reaction between NO and the reduced Pt at the leading edge of the front where the hydrogen is depleted, and not from the reaction between the NO_x and H_2, since we believe that the high NO_x:H_2 ratios required for N_2O formation are not achieved in the front. The NO and NO_2 profiles are due to simple desorption and their subsequent reaction in the front.

Acknowledgements

The authors thank the Indiana 21st Century Research and Technology Fund and Cummins Inc. for the financial support of this work.

References

[1] Control of air pollution from new motor vehicles: heavy-duty engine and vehicle standards and highway diesel fuel sulfur control requirements, U.S. EPA, 40 CFR Part 69, 80 and 86.
[2] W.S. Epling, L.E. Campbell, A. Yezerets, N.W. Currier, J.E. Parks, Catal. Rev. 46 (2004) 163.
[3] Y. Kosaki, A. Miyamoto, Y. Murakami, Chem. Lett. 8 (1979) 935.
[4] J. Siera, P. Cobden, K. Tanaka, B.E. Nieuwenhuys, Catal. Lett. 10 (1991) 335.
[5] L. Cumaranatunge, S.S. Mulla, A. Yezerets, N.W. Currier, W.N. Delgass, F.H. Ribeiro, J. Catal. 246 (2007) 29.
[6] K.S. Kabin, R.L. Muncrief, M.P. Harold, Catal. Today 96 (2004) 79.
[7] A. Amberntsson, H. Persson, P. Engstrom, B. Kasemo, Appl. Catal. B 31 (2001) 27.
[8] Z. Liu, J.A. Anderson, J. Catal. 224 (2004) 18.
[9] S. Balcon, C. Potvin, L. Salin, J.F. Tempere, G. Djega-Mariadassou, Catal. Lett. 60 (1999) 39.
[10] S. Poulston, R.R. Rajaram, Catal. Today 81 (2003) 603.
[11] L. Castoldi, I. Nova, L. Lietti, E. Tronconi, P. Forzatti, Top. Catal. 42–43 (2007) 189.
[12] R. Burch, P.J. Millington, Catal. Today 29 (1996) 37.
[13] T. Maunula, J. Ahola, H. Hamada, Appl. Catal. B 26 (2000) 173.
[14] I. Nova, L. Lietti, L. Castoldi, E. Tronconi, P. Forzatti, J. Catal. 239 (2006) 244.
[15] P. Forzatti, L. Castoldi, I. Nova, L. Lietti, E. Tronconi, Catal. Today 117 (2006) 316.
[16] N.W. Cant, I.O.Y. Liu, M.J. Patterson, J. Catal. 243 (2006) 309.
[17] H. Abdulhamid, E. Fridell, M. Skoglundh, Appl. Catal. B 62 (2006) 319.
[18] H. Abdulhamid, E. Fridell, M. Skoglundh, Top. Catal. 30/31 (2004) 161.
[19] T. Szailer, J.H. Kwak, D.H. Kim, J.C. Hanson, C.H.F. Peden, J. Szanyi, J. Catal. 239 (2006) 51.
[20] J.P. Breen, C. Rioche, R. Burch, C. Hardacre, F.C. Meunier, Appl. Catal. B 72 (2007) 178.
[21] J.A. Pihl, J.E. Parks, C.S. Daw, T.W. Root, SAE Technical Papers, 2006-01-3441 (2006).
[22] J.E. Benson, M. Boudart, J. Catal. 4 (1965) 704.
[23] S.S. Mulla, N. Chen, L. Cumaranatunge, W.N. Delgass, W.S. Epling, F.H. Ribeiro, Catal. Today 114 (2006) 57.
[24] I. Nova, L. Castoldi, L. Lietti, E. Tronconi, P. Forzatti, Top. Catal. 42–43 (2007) 21.
[25] R.E. Hayes, S.T. Kolaczkowski, Catal. Today 47 (1999) 295.
[26] M. Abul-Milh, H. Westberg, Top. Catal. 42–43 (2007) 209.
[27] M. Shelef, J.H. Jones, J.T. Kummer, K. Otto, E.E. Weaver, Environ. Sci. Technol. 5 (1971) 790.
[28] A. Lindholm, N. Currier, A. Yezerets, L. Olsson, Top. Catal. 42–43 (2007) 83.
[29] K. Otto, M. Shelef, J.T. Kummer, J. Phys. Chem. 74 (1970) 2690.
[30] W.S. Epling, J.E. Parks, G.C. Campbell, A. Yezerets, N.W. Currier, L.E. Campbell, Catal. Today 96 (2004) 21.
[31] L. Lietti, P. Forzatti, I. Nova, E. Tronconi, J. Catal. 204 (2001) 175.
[32] W.S. Epling, A. Yezerets, N.W. Currier, Appl. Catal. B 74 (2007) 117.